Optimal Design of a Novel V-Type Interior Permanent Magnet Motor with Assisted Barriers for the Improvement of Torque Characteristics

Wenliang Zhao[1], Fei Zhao[1], Thomas A. Lipo[2], *Life Fellow, IEEE*, and Byung-Il Kwon[1]

[1]Department of Electronic Systems Engineering, Hanyang University, Ansan 426-791, Korea
[2]Department of Electrical and Computer Engineering, University of Wisconsin-Madison, Madison, WI 53706-1691 USA

This paper performs a study on the optimal design of V-type interior permanent magnet motors (VIPMMs), in which the rotor is equipped with assisted barriers for the improvement of average torque and torque ripple. The approach differs from the conventional interior permanent magnet motors, in which the reluctance torque due to saliency reaches a maximum value at a current phase angle located 45 electrical degrees with respect to the maximum value obtained from the magnetic torque produced by the rotor magnets. The adoption of assisted barriers is employed to improve the torque production by creating rotor asymmetry to allow the reluctance torque and the magnetic torque reach a maximum value near or at the same current phase angle. To evaluate the contribution, the frozen permeability method is utilized to segregate the torque into its reluctance and magnetic torque components. First, an iterative optimization is performed on a concept design of a 6/4 VIPMM for demonstrating the design principle based on finite element method. Then, the VIPMM is further optimized by algorithms, such as the kriging method and genetic algorithm for improving the torque characteristics and efficiency. As a result, the optimal VIPMM with assisted barriers shows the substantially improved performance compared with a conventional design.

Index Terms— **Finite-element method (FEM), frozen permeability method (FPM), genetic algorithm (GA), magnetic torque, optimal design, torque, torque ripple, V-type interior permanent magnet motors (VIPMMs).**

I. Introduction

In RECENT years, permanent magnet brushless motors have been comprehensively investigated for many applications due to their superior torque density/shear stress [1]. In general, the representative motors can be classified as surface-mounted permanent magnet motor (SPMM) and interior permanent magnet motor (IPMM). The SPMM is known to have high-torque density and efficiency resulting from the magnetic torque, and the IPMM offers the advantages, such as high torque density and efficiency as well as extended speed range benefitting from both of the magnetic torque and reluctance torque [2]. Furthermore, it has been shown that the V-type IPMM (VIPMM) contains a higher saliency ratio and lower permanent magnet (PM) losses than the flat type, making it more suitable for high-speed applications especially for electric vehicles [3]. In general, however, further improved performance is always desirable.

An extensive literature with various techniques can be found for improving the performance of IPMMs [4]. In particular, the flux barrier design has been recognized as an effective solution when applied to the reduction of torque ripple rather than the improvement of average torque [5]. It is well known that one of the significant features in IPMMs is the presence of magnetic saliency, which contributes to the production of reluctance torque, resulting in enhanced torque and efficiency combining with the magnetic torque from the rotor magnets. By convention, an elegant d–q rotor frame equivalent circuit can be developed for analyzing the torque components using Park transformation, where it is displayed that the magnetic torque and the reluctance torque reach the maximum value at different current phase angles theoretically by 45 electrical degrees with respect to each other. Consequently, the resultant torque is obtained as the vector sum of the two components rather than the algebraic sum. Hence, only a portion of each torque component is effectively utilized in any known IPMM design previously reported.

In this paper, a novel VIPMM with assisted barriers between two adjacent poles is proposed for improving torque characteristics by making the magnetic torque and the reluctance torque reach their maximum near or at the same current phase angle. To provide visible insights to the contribution, the frozen permeability method (FPM) is utilized to separate the torque into the reluctance torque and magnetic torque based on a 2-D time stepping finite element method (FEM) [6]. First, an iterative optimization is performed on the concept design of a 6/4 VIPMM for demonstrating the design principle. Then, the VIPMM is optimized by algorithms such as the kriging method and a genetic algorithm (GA) for further improving the torque characteristics and efficiency. The consequent optimal results show that the performance of the optimal motor with assisted barriers has been substantially improved when compared with that of a conventional design.

II. Concept Design

A. Typical Torque Characteristics of VIPMM

Fig. 1(a) shows the configuration of the conventional VIPMM. The stator has six slots with concentrated winding. The ferrite magnets buried in the rotor are arranged as V shape.

Manuscript received March 7, 2014; revised June 3, 2014; accepted June 3, 2014. Date of current version November 18, 2014. Corresponding author: B.-I. Kwon (e-mail: bikwon@hanyang.ac.kr).

Color versions of one or more of the figures in this paper are available online at http://ieeexplore.ieee.org.

Digital Object Identifier 10.1109/TMAG.2014.2330339

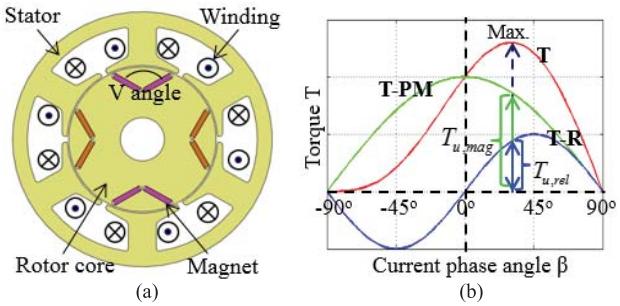

Fig. 1. (a) Topology of the conventional VIPMM. (b) Typical torque characteristics. T: total torque. T-PM: magnetic torque. T-R: reluctance torque.

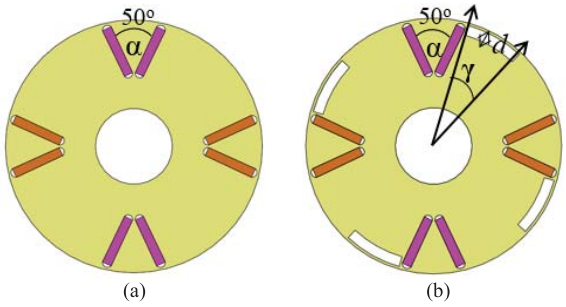

Fig. 2. V-type IPM motors in concept design. (a) Basic motor. (b) Proposed motor with assisted barriers.

By convention, the electromagnetic torque obtained from the d–q rotating reference frame can be expressed as

$$T = \frac{3p}{2}\left[\lambda_{\text{pm}} I_a \cos\beta + \frac{1}{2}(L_d - L_q) I_a^2 \sin 2\beta\right] \quad (1)$$

where p is the number of pole pairs, β is the spatial angle of the stator current vector measured with respect to the q-axis, L_d and L_q are the inductances of the d- and q-axes, respectively, I_a is the peak value of phase current and λ_{pm} is the peak fundamental value of magnet flux linking the stator windings. The first term in (1) is termed the magnetic torque, while the second term is the reluctance torque.

FPM is utilized to separate the torque into the reluctance torque and magnetic torque based on FEM. The resultant torque was first obtained with both PM and current excitations. Then, the magnets were removed and the reluctance torque was determined. The magnetic torque was then calculated by subtracting the reluctance torque from the resultant torque. The typical torque characteristics based on (1) are shown in Fig. 1(b). To evaluate the contribution of the proposed design concept, a utilization factor (UF) is defined as the ratio between the utilized magnetic or reluctance torque component contributing to the maximum torque and its corresponding peak torque component, which can be expressed as

$$\text{UF}_{\text{mag}} = \frac{T_{u,\text{mag}}}{T_{\text{pk,mag}}}, \qquad \text{UF}_{\text{rel}} = \frac{T_{u,\text{rel}}}{T_{\text{pk,rel}}} \quad (2)$$

where $T_{u,\text{mag}}$ and $T_{u,\text{rel}}$ are the utilized magnetic torque and the utilized reluctance torque that contribute to the maximum resultant torque, as shown in Fig. 1(b), respectively. $T_{\text{pk,mag}}$ and $T_{\text{pk,rel}}$ are the peak values of each torque component.

TABLE I
SPECIFICATION OF THE INVESTIGATED MOTOR

Item	Unit	Value
Number of magnet poles	-	4
Number of stator slots	-	6
Stator outer diameter	mm	88
Stator inner diameter	mm	51
Airgap length	mm	0.5
Rotor outer diameter	mm	50
Rotor inner diameter	mm	15
Lamination axial length	mm	52
Remanence of Ferrite PM	T	0.41

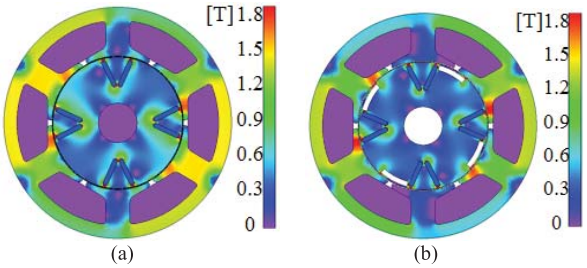

Fig. 3. Magnetic flux density distribution. (a) Basic motor. (b) Proposed motor.

B. Concept Design

As opposed to conventional design techniques, the improvement of the torque production in this paper is achieved by making the reluctance torque and the magnetic torque reach their maximum near or at the same current phase angle. To demonstrate the design principle, an iterative optimization can be first performed on the concept design.

Fig. 2 shows the motors that were investigated. The basic motor with the V-angle of 50° is shown in Fig. 2(a), and the proposed motor with the design variable selected as the open angle of the assisted barrier γ is shown in Fig. 2(b). The motor specification is listed in Table I. The rated speed is 4800 r/min. The torque characteristics are analyzed by feeding with three-phase sinusoidal current excitation at the current density of 3 Arms/mm^2. The optimization criterion is to make the UF of each torque component as unity. By an iterative optimization process, a value of UF as unity occurs at $\gamma = 27°$.

The magnetic flux density distribution for both motors in Fig. 3 shows that the proposed motor with assisted barriers improves the magnetic flux density distribution as compared with the basic motor. Fig. 4 shows the torque characteristics of both motors. The two torque components reach their maximum values at different current phase angles in basic motor, as shown in Fig. 4(a), while it shows that the two torque components of the proposed motor reach the maximum values at the same current phase angle, which improves the resultant torque dramatically, as shown in Fig. 4(b). The maximum resultant torque for the proposed motor has increased over 35.5% from that of the basic motor demonstrating a superior result using the same amount of magnet material. The efficiency has also increased by 6.3% due to the improvement of

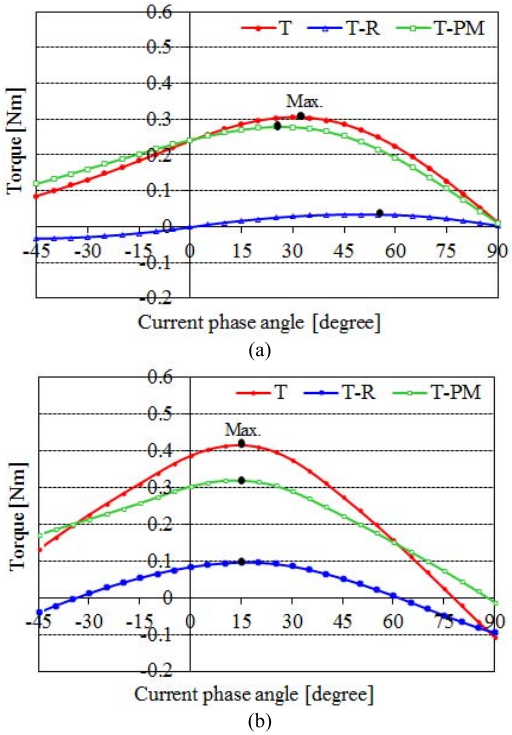

Fig. 4. Torque characteristics. T: Resultant torque, T-PM: Magnetic torque. T-R: Reluctance torque. (a) Basic motor. (b) Proposed motor.

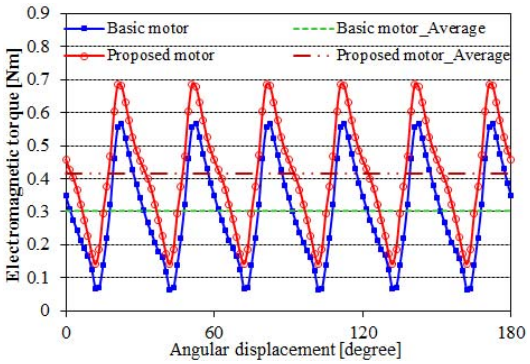

Fig. 5. Electromagnetic torque of the basic and proposed motors.

torque and the reduction of iron loss. The efficiency is herein defined as

$$\eta = \frac{P_{\text{out}}}{P_{\text{out}} + P_{\text{copper}} + P_{\text{iron}}} \tag{3}$$

where P_{out} is the output power, P_{copper} is the copper loss, and P_{iron} is the iron loss in the stator and rotor core.

Fig. 5 shows the comparison of electromagnetic torque. The torque ripple factor is defined as the ratio of peak-to-peak torque value to average torque value as

$$K_t = \frac{T_{\max} - T_{\min}}{T_{\text{AVG}}}. \tag{4}$$

The torque ripple factor of the proposed motor is decreased by 21.7%, and the detailed data is summarized in Table II.

TABLE II
COMPARISON OF PERFORMANCE DATA IN CONCEPT DESIGN

Item	Unit	Basic motor	Proposed motor
Max. torque (Average)	Nm	0.307	0.416
UF of reluctance torque	%	83.1	100
UF of magnetic torque	%	99.2	100
Torque ripple	%	166.1	131.2
Output power	W	154.3	209.1
Copper loss	W	9.6	
Iron loss	W	19.56	15.28
Efficiency	%	84.1	89.4

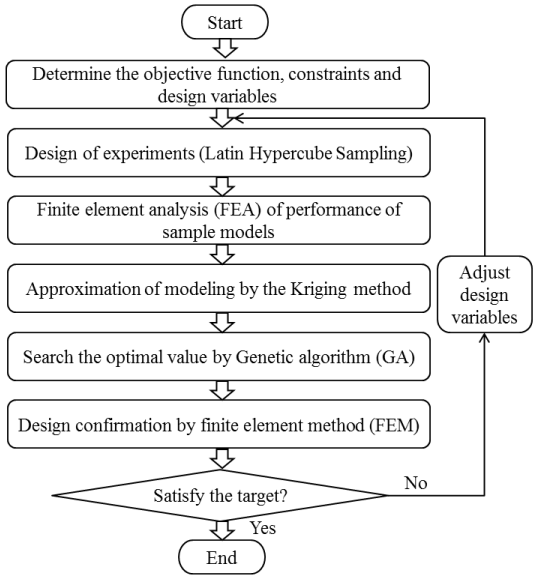

Fig. 6. Optimal design process.

III. OPTIMAL DESIGN

A. Optimal Design Process

Based on the proposed motor design strategy, an optimal design was performed to further improve torque and efficiency, as shown in Fig. 6. First, the objective functions, constraints, and design variables were determined. Then, the latin hypercube sampling was applied in a design of experiment process for the selection of sampling points and the kriging method performed for the approximation modeling. Using the GA, optimal points for the design variables were obtained. Finally, the optimal design results were verified by FEM.

B. Objective Function, Constraints, and Design Variables

The objective functions for maximizing the average torque and efficiency are shown in (5). The constraints are the magnet volume and UF of torque components as shown in (6). The design variables are shown in Fig. 2(b) and (7). α is the V angle of magnet poles, γ is the span angle of the assisted

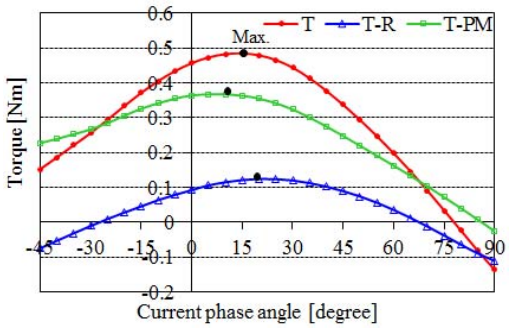

Fig. 7. Torque characteristics of the optimized motor. T: Resultant torque. TPM: Magnetic torque. T-R: Reluctance torque.

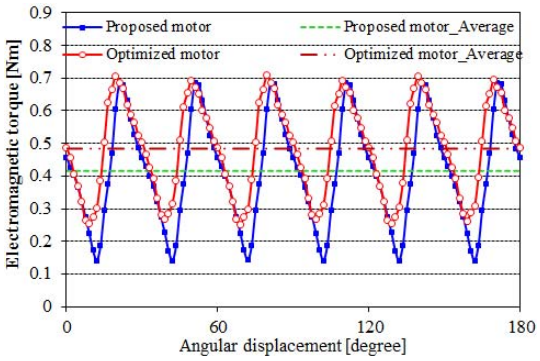

Fig. 8. Comparison of electromagnetic torque.

barrier and d is the thickness of the assisted barrier

Objective functions:

Maximize the average torque and efficiency (5)

Constraints:

Magnet volume $= 7.5\ \text{cm}^3$

UF of reluctance torque $\geq 97\%$

UF of magnetic torque $\geq 97\%$ (6)

Design variables:

$45° \leq \alpha$ (V angle of magnets) $\leq 120°$

$25° \leq \gamma$ (Span angle of assisted barrier) $\leq 40°$

1 mm $\leq$ d (Thickness of assisted barrier) ≤ 4 mm. (7)

C. Optimal Design Results

The optimal design variables for the optimized motor are $\alpha = 83°$, $\gamma = 26°$, and $d = 3.4$ mm, respectively. Fig. 7 shows the torque characteristics of the optimized motor. The reluctance torque and the magnetic torque reach a maximum near the same current phase angle. The comparison of electromagnetic torque (max) between the proposed motor and the optimized motor is shown in Fig. 8. Compared with the proposed motor, the maximum torque of the optimized motor is increased by 16.6% and the efficiency is increased by 1.9%, while the torque ripple is decreased by 18.7%. The comparison of detailed performance data between the proposed motor and the optimized motor are listed in Table III.

TABLE III
COMPARISON OF PERFORMANCE DATA IN OPTIMAL DESIGN

Item	Unit	Proposed motor	Optimized motor
Max. torque (Average)	Nm	0.416	0.485
UF of reluctance torque	%	100	97.8
UF of magnetic torque	%	100	98.8
Torque ripple	%	131.2	106.7
Output power	W	209.1	243.8
Copper loss	W	9.6	
Iron loss	W	15.28	14.20
Efficiency	%	89.4	91.1

IV. CONCLUSION

This paper has proposed a new rotor optimal design strategy for VIPMMs. The proposed motor adopts assisted barriers between two adjacent magnet poles aiming at improving the torque characteristics by making the reluctance torque and the magnetic torque reach a maximum value near or at the same current phase angle. As the results show, the final optimized motor with assisted barriers demonstrates good performance with the improved torque and efficiency as well as reduced torque ripple when compared with a conventional design. It can be concluded that the proposed technique is an effective and competitive approach to the design of high performance PM motors where magnetic saliency exists.

ACKNOWLEDGMENT

This work was supported by the BK21PLUS Program through the Ministry of Education, National Research Foundation of Korea.

REFERENCES

[1] J. J. H. Paulides, B. L. J. Gysen, K. J. Meessen, Y. Tang, and E. A. Lomonova, "Influence of multiple air gaps on the performance of electrical machines with (semi) Halbach magnetization," *IEEE Trans. Magn.*, vol. 47, no. 10, pp. 2664–2667, Oct. 2011.

[2] F. Parasiliti, M. Villani, S. Lucidi, and F. Rinaldi, "Finite-element-based multiobjective design optimization procedure of interior permanent magnet synchronous motors for wide constant-power region operation," *IEEE Trans. Ind. Electron.*, vol. 59, no. 6, pp. 2503–2514, Jun. 2012.

[3] P. Zhang, D. M. Ionel, and N. A. O. Demerdash, "Morphing parametric modeling and design optimization of spoke and V-type permanent magnet machines by combined design of experiments and differential evolution algorithms," in *Proc. IEEE Energy Convers. Congr. Expo. (ECCE)*, Sep. 2013, pp. 5056–5063.

[4] R. Akaki, Y. Takahashi, K. Fyjiwara, M. Matsushita, N. Takahashi, and M. Morita, "Effect of magnetic property in bridge area of IPM motors on torque characteristics," *IEEE Trans. Magn.*, vol. 49, no. 5, pp. 2335–2338, May 2013.

[5] P. Alotto, M. Barcaro, N. Bianchi, and M. Guarnieri, "Optimization of interior PM motors with Machaon rotor flux barriers," *IEEE Trans. Magn.*, vol. 47, no. 5, pp. 958–961, May 2011.

[6] W. Q. Chu and Z. Q. Zhu, "Average torque separation in permanent magnet synchronous machines using frozen permeability," *IEEE Trans. Magn.*, vol. 49, no. 3, pp. 1202–1210, Mar. 2013.